SOUTHWEST RESEARCH INSTITUTE
8500 Culebra Road, San Antonio 6, Texas

Department of Mechanical Sciences
Engineering Analysis Section

LIQUID SLOSHING IN SPHERICAL TANKS

by

H. Norman Abramson
Wen-Hwa Chu
Luis R. Garza

Technical Report No. 2
Contract No. NAS8-1555
SwRI Project No. 6-1072-2

Prepared for

National Aeronautics and Space Administration
George C. Marshall Space Flight Center
Huntsville, Alabama

15 March 1962

APPROVED:

H. Norman Abramson

H. Norman Abramson, Director
Department of Mechanical Sciences

INTRODUCTION

The design of large liquid propellant rockets and booster systems involves consideration of various tank configurations and the forces and moments resulting from sloshing of the contained liquids. In view of the customary high fineness ratio of such vehicles, most emphasis has been placed on cylindrical tanks (1, 2)*; however, in many instances where high strength-weight ratios are of great importance, in combination with other factors, spherical tanks have been employed. Knowledge of sloshing behavior in spherical tanks is considerably more limited than for cylindrical tanks, partially because of the increased complexity of theoretical analysis.

Virtually the only theoretical analysis available for spherical tank sloshing is that of Budiansky (3) and, although somewhat sophisticated integral equation techniques were employed, the analysis is strictly valid only for the cases of the nearly empty, one-half full, and nearly full tank. The lowest three or four natural frequencies of the liquid free surface motion, over the entire range of liquid depths, have been determined experimentally by McCarty and Stephens (4), confirming the theoretical values predicted by Budiansky (3) for the nearly empty and one-half full conditions.

---

* Numbers in parenthesis refer to the References given at the end of the paper.

The purpose of the present paper is to present experimental data on the forced vibration characteristics of partially filled unbaffled and baffled spherical tanks. For the unbaffled tank, comparisons are made with previously measured natural frequencies (4) and with the predictions of the Budiansky analysis (3). For the baffled tanks, comparisons are made with the force response predicted from an equivalent mechanical model.*

---

* This analogy was developed by one of the authors, W. H. Chu, and is presented in the Appendix to this paper.

EXPERIMENTAL RESULTS

Experimental Facilities and Procedures.

The SwRI slosh test facility, previously described in (5), was modified to accommodate a spherical tank approximately 15 inches in diameter (internal diameter of 14.5 inches). The tank was fabricated in two halves from 1020 steel sheet by spinning and was assembled by means of an equatorial flange; the tank was intended to be rigid. Instrumentation consisted of a dynamometer system for measurement of total force and moment response (5) and a small array of pressure cells. The excitation was translational in the horizontal direction.

For the studies of the effects of baffling, six perforated ring baffles of 23% open area were employed. The baffles were fabricated from 0.016 in. thick perforated brass sheet having 0.020 in. diameter holes and were mounted in the tank so as to form great circles at 30° to each other. The baffle width was 2.06 in. (baffle width to radius ratio of 28.5%). Tests were conducted with the baffles in two different orientations; the horizontal orientation is shown in Figure 1*. The vertical orientation was formed simply by rotating the sphere 90°, so as to form lines of longitude. In both orientations, the same cross-section of the sphere (containing one of the baffles) is normal to the translational excitation axis; hence, in Figure 1 the axis of translation is normal to the page.

---

* Certain of the pressure cells may also be seen in this figure.

Total Force Response - Unbaffled Tank.

As a matter of simple comparison, previous data (3,4) for first mode natural liquid frequency variation with depth is shown, together with present SwRI data, in Figure 2. The natural frequency ω_n is given in terms of the non-dimensional parameter $\omega_n^2 d/a$, where a represents a vertical acceleration field.

Total force response, in terms of dimensionless amplitude and phase angle, is shown as a function of the frequency parameter at various liquid depths in Figures 3-6. The vertical line in each plot represents the fundamental liquid resonant frequency.

The effect of different excitation amplitudes X_o, is shown in Figures 4, 5, and 6. Lower values of excitation amplitude generally appear to produce somewhat greater response for frequencies less than the fundamental, and lower response for frequencies greater than the fundamental. Figure 6, corresponding to a nearly full tank, shows a prominent peak in response only for the lower excitation amplitude, the higher excitation amplitude apparently introducing sufficiently large amplitudes of free surface motions that the damping becomes quite high.

Figures 3, 4, and 5 also contain theoretical force response curves as obtained from Budiansky's analysis (3)* . The in-phase portions of these

---

* Since the theory is strictly valid only for $h/d = 0$ and 0.50, the values for $h/d = 0.25$ and 0.75 were obtained by estimating values from the interpolated curves given in (3), with consequent inaccuracies.

curves generally show good agreement between theory and experiment, the out-of-phase portions show somewhat poorer agreement, with the experimental data corresponding to lower excitation amplitudes being much closer to the theoretical curves than that corresponding to the higher excitation amplitude. The effects of large excitation amplitudes are therefore again emphasized.

As a further comparison between the Budiansky theory (3) and the experimental response data, experimentally determined pressure distribution data for $h/d = 0.50$ and $X_o/d = 0.00828$ (high excitation amplitude) was integrated to give total force, as shown in Figure 4. The agreement with the Budiansky theory is good; this, however, is probably only a fortuitous circumstance because the pressure data is not sufficiently detailed to permit accurate integration (see below).

Pressure Distribution - Unbaffled Tank.

Figure 7 shows experimental wall pressure distribution data, similar to that presented previously for cylindrical tanks (6). The wall pressures are given in non-dimensional form as a function of pressure cell location z/d (measured vertically from the tank bottom), with excitation frequency as a parameter. The pressures are, of course, those normal to the tank wall. A few measured values were also obtained along lines of latitude at $z/d = 0.5$, 0.375, and 0.25. As is evident from Figure 7, there are not sufficient measured values to

insure accurate pressure distribution curves, particularly as required for integration to obtain total force response (see above), the data given is therefore useful primarily to indicate trends and magnitudes. The magnitudes of the pressures are, incidentally, considerably higher than for an equivalent cylindrical tank (6).

Total Force Response - Baffled Tank.

Total force response data for the spherical tank with either horizontal or vertical perforated ring baffles (Figure 1) are shown in Figures 8 and 9. Both baffle orientations provide large force amplitude damping, with the horizontal arrangement being considerably more effective in this respect than the vertical arrangement. This is expected from the orientation of the rings with respect to the liquid free surface.

For rather full unbaffled tanks ($h/d \geq 0.75$), as may be inferred from Figure 6, the peak force response is sufficiently small so as to be more like that of a well-baffled tank. In fact, for $h/d = 0.875$ and $X_o/d = 0.00828$, the force response for the unbaffled tank and for the tank with either horizontal or vertical baffles are virtually the same. Hence, one could conclude that baffling is required in spherical tanks only for $h/d \leq 3/4$, at the excitation amplitudes considered. For very shallow liquid depths, say $h/d = 0.25$, the horizontal baffle orientation provides almost complete suppression of the force response. As may be noted particularly from both Figures 8 and 9, the presence of baffles also has a significant effect in lowering the fundamental liquid resonant frequency.

In order to place these data on baffle effectiveness on a somewhat more quantitative basis, an attempt was made to obtain values of damping factor g. The half-bandwidth procedure applied to the experimental force response peaks, as employed in previous work (5), could give g values in only a few instances, however, because of the rather large damping provided by both of these baffle configurations. As noted above, for large depths (such as h/d = 0.875) the unbaffled tank response is so highly damped in itself that baffling has no additional effect; for shallow depths (such as h/d = 0.25) the damping provided by either baffle configuration is also so large as to suppress completely the liquid free surface motion. Even for the half-full case of h/d = 0.50, the horizontal baffle configuration is so effective as to virtually eliminate the response peak (Fig. 8); at h/d = 0.75 (X_o/d = 0.00828) the horizontal baffle yields a damping factor of g = 0.65, which is a quite large value (Fig. 9). The vertical baffle configuration yields a damping factor g = 0.31 for depths of h/d = 0.50 and 0.75, for an excitation amplitude of X_o/d = 0.00828 (Figs. 8 and 9). It is emphasized that these g values are given here primarily for demonstrating the orders of magnitude involved and for comparison with similar data for cylindrical tanks (5).

Equivalent Mechanical Model.

In order to be able to incorporate liquid force response data into vehicle dynamic analyses, recourse is often made to representation by

an equivalent mechanical model. By incorporating viscous dashpots into the mechanical elements of the model, it is therefore possible to employ such models for representation of baffled tanks*.

Using the g values given in the preceding section, force response curves have been calculated from the mechanical model for the spherical tank with vertical baffles with h/d = 0.50 and 0.75, as shown in Figures 8 and 9. In both cases, the predicted values of the peak response are considerably below the measured values, while the value of the frequency parameter at which the peak occurs is considerably higher for the calculated data than for the measured data. Recognizing that the g values obtained from the experimental data are probably not too accurate, the case of vertical baffles at h/d = 0.50 was also calculated for a smaller value of damping (g = 0.25), rather than the value of g = 0.31 originally obtained, with consequent better agreement in peak value with the measured data (see Fig. 8).

As has been noted in the earlier discussion of this paper, sloshing in spherical tanks appears to involve much larger free surface amplitudes than is customarily observed in cylindrical tanks, even at very low excitation amplitudes, so that an essentially larger degree of nonlinearity is present. This is particularly evidenced by the differences between the measured force response and that predicted by theory, and the very

---

* See (7) for a discussion of mechanical models for cylindrical tanks. The derivation of the mechanical model for the present case of a spherical tank is given in the Appendix to this paper.

large damping and reduction in liquid natural frequencies produced by both baffle arrangements. Thus, while the response curves calculated from the equivalent mechanical model representation, based on damping values obtained from the measured data, are not in particularly good agreement with the measured force response, the disagreement is probably no more than should be expected from a linearized representation.

DISCUSSION AND CONCLUSIONS

The results of this study would appear to reveal several important features of sloshing in spherical tanks. For example, while the basic predictions of the Budiansky theory (3) have been confirmed, particularly for liquid natural frequency, the force response is quite dependent on the magnitude of the excitation amplitude. Hence, large amplitude liquid free surface motions are more easily excited and appear to be of more importance in modifying the total force response in spherical tanks than in cylindrical tanks.

Perforated ring baffles oriented horizontally appear to be quite effective in providing force amplitude damping, with significant lowering of the fundamental resonant frequency. No baffling is apparently required for large liquid depths, say $h/d > 3/4$. A linear mechanical model representation for baffled tanks would appear to be satisfactory only for order of magnitude estimates.

ACKNOWLEDGEMENTS

The authors wish to thank Mr. Daniel D. Kana for his assistance in several instances and Mr. Gilbert R. Rivera for performing computations and preparing the figures.

REFERENCES

1. Cooper, R. M., "Dynamics of Liquids in Moving Containers", ARS Journal, 30, pp. 725-729, August 1960.

2. Abramson, H. N., "Liquid Dynamic Behavior in Rocket Propellant Tanks", AIA/ONR Symposium on Structural Dynamics of High Speed Flight, pp. 287-318, Los Angeles, April 1961 (also see, Astronautics, 6, pp. 35-37 ff., March 1961.)

3. Budiansky, B., "Sloshing of Liquids in Circular Canals and Spherical Tanks", Journal of Aero/Space Sciences, 27, pp. 161-173, March 1960.

4. McCarty, J. L. and Stephens, D. G., "Investigation of the Natural Frequencies of Fluids in Spherical and Cylindrical Tanks", NASA Tech. Note D-252 (May 1960).

5. Abramson, H. N., and Ransleben, G. E., Jr., "Simulation of Fuel Sloshing Characteristics in Missile Tanks by Use of Small Models", ARS Journal, 30, pp. 603-612, July 1960.

6. Abramson, H. N., and Ransleben, G. E., Jr., "A Note on Wall Pressure Distributions During Sloshing in Rigid Tanks", ARS Journal, 31, pp. 545-547, April 1961.

7. Abramson, H. N., Chu, W. H., and Ransleben, G. E., Jr., "Representation of Fuel Sloshing in Cylindrical Tanks by an Equivalent Mechanical Model", ARS Journal, 31, pp. 1697-1705, December 1961.

APPENDIX - EQUIVALENT MECHANICAL MODEL FOR SLOSHING IN A SPHERICAL TANK

Consider a pendulum oscillating about the y-axis through the centroid of a spherical tank, as shown in Figure A-1. Equilibrium of forces yields

$$F_{x,n} = T_n \sin\theta_n \cong T_n \theta_n \qquad \text{(on tank wall)} \qquad \text{(A-1)}$$

$$\sum F_{r,n} = m_n a \cos\theta_n - T_n - (m_n \ddot{x}_T \sin\theta_n) = 0 \qquad \text{(A-2)}$$

$$\sum F_{\theta,n} = -m_n a \sin\theta_n - (m_n \ddot{x}_T)\cos\theta_n - m_n l_n \ddot{\theta}_n = 0 \qquad \text{(A-3)}$$

where T_n is the tension in the n^{th} pendulum, m_n is the mass of the n^{th} pendulum, and a is the effective gravitational acceleration. Then with

$$T_n \cong m_n a$$

$$m_n l_n \ddot{\theta}_n + m_n a \theta_n \cong -m_n \ddot{x}_T$$

$$\theta_n = \frac{\omega^2 m_n x_T}{m_n a - m_n l_n \omega^2} = \frac{\omega^2 (2x_T/d)}{(\omega_n^2 - \omega^2)(2l_n/d)}, \quad \theta_0 = \frac{\omega^2 x_T}{a}$$

$$\omega^2 = a/l_n$$

$$x_T = l\theta_y + x_b$$

we have

$$F_x = \sum_{n=0}^{\infty} F_{x,n} = \sum_{n=1}^{\infty} \frac{m_n a \omega^2 (2x_T/d)}{(\omega_n^2 - \omega^2)(2l_n/d)} + M_0 \omega^2 x_T$$

$$= M_0 \omega^2 x_T + \sum_{n=1}^{\infty} m_n \omega^2 x_T + \sum_{n=1}^{\infty} \frac{\omega^2 m_n x_T}{\left(\frac{\omega_n^2}{\omega^2} - 1\right)} \qquad \text{(A-4)}$$

With $y_T = -l\theta_x + y_b$, a similar expression for F_y can be obtained.

From Budiansky's analysis (3), the sloshing force on the tank can be derived from Lagrange's equation,

$$F_s = -M_L\ddot{U} - \rho_L \sum \beta_n \ddot{A}_n \tag{A-5}$$

where

$$M_L = \rho_L \frac{\pi}{3}\left(\frac{d^3}{4} + \frac{3d^2}{4} z_F - z_F^3\right)$$

$$\beta_n = \frac{\omega_n^2}{a}\int_F \phi_n \, dS = \pi b^2 \Omega_n \frac{2b}{a}\int_0^{b=1} \varphi_n \rho^2 \, d\rho$$

$$\alpha_n = \int_F \phi_n^2 \, dS = \pi b^2 \int_0^{b=1} \varphi_n^2(\rho_2)\rho_2 \, d\rho_2$$

$$\ddot{A}_n = \frac{\frac{a}{\omega_n^2}\cdot\frac{\beta_n}{\alpha_n}\ddot{U}}{\frac{\omega_n^2}{\omega^2} - 1}$$

$$\Omega_n = \frac{\omega_n^2 d}{2a}$$

we have

$$M_L = M_0 + \sum_{n=1}^{\infty} m_n = \rho_L V_L$$

$$m_n = \frac{\rho_L \beta_n^2 d/\alpha_n}{2\Omega_n}$$

so that

$$F_x = M_L\omega^2 x_T + \rho_L \omega^2 x_T \sum_{n=1}^{\infty} \frac{\beta_n^2 d/\alpha_n}{2\Omega_n\left(\frac{\omega_n^2}{\omega^2} - 1\right)} \tag{A-6}$$

It follows that

$$F_x = -\sum_{n=0}^{\infty} m_n a = -M_L a$$

as required.

Since the angle θ_n may be either in-phase or out-of-phase with x_T, a collection of conical pendulums hinged at the centroid of the sphere may collide during motion. Therefore, the set of pendulums will be hinged along the y-axis, as shown in Figure A-2. The twisting moment about the centroid of the sphere will be zero if each pendulum is now divided into two pendulums of equal mass but at equal and opposite distances $\bar{\epsilon}_n$ from the center (these distances are sufficiently large so that the pendulums will not collide with one another or the tank; $\frac{2l_n}{d} = \frac{1}{\Omega_n} < \frac{1}{\Omega_1} \leq 1$). An identical set of pendulums is hinged along the x-axis.

To account for the presence of damping, the hinge point of each pendulum is replaced by an idealized viscous joint which produces a restoring moment $\mu_n \dot{\theta}_n$ while transmitting a moment $\eta_n \mu_n \dot{\theta}_n$. This damping moment produces a shear force in the pendulum arm and at the point mass m_n, opposing the motion and having the magnitude $V_n = \frac{\mu_n \dot{\theta}_n}{l_n}$. Hence,

$$\sum F_\theta = -m_n l_n \ddot{\theta}_n - m_n a \sin\theta_n - (m_n \ddot{x}_T)\cos\theta_n - \frac{\mu_n \dot{\theta}_n}{l_n} = 0 \qquad \text{(A-7)}$$

Now, let

$$\mu_n = m_n l_n^2 \omega_n \eta_n$$

$$\theta_n = \frac{\omega^2 x_T}{(\omega_n^2 - \omega^2 + i\omega\omega_n\eta_n) l_n} = \frac{x_T/l_n}{(\frac{\omega_n^2}{\omega^2} - 1) + i\eta_n \frac{\omega_n}{\omega}}$$

The horizontal force is then

$$F_x = M_0 \omega^2 x_T + \sum_{n=1}^{\infty} \frac{m_n \omega_n^2 x_T}{\left(\frac{\omega_n^2}{\omega^2} - 1 + i g_n \frac{\omega_n}{\omega}\right)} \qquad \text{(A-8)}$$

and the moments on the tank provided by the viscous joints are

$$M_y = -\sum_{n=1}^{\infty} \eta_n \mu_n \frac{\dot{\theta}_n}{I_n} = -\sum_{n=1}^{\infty} \eta_n m_n l_n^2 \omega_n g_n \frac{\dot{x}_T / l_n}{\left(\frac{\omega_n^2}{\omega^2} - 1\right) + i g_n \frac{\omega_n}{\omega}}$$

$$M_x = -\frac{M_y}{\dot{x}_T} \dot{y}_T$$

If each viscous joint is eliminated by adding a pair of dashpots which produce a pure moment on the tank equal and opposite to the damping moment on the pendulum, then $\eta_n = 1$. The values of g_n are, of course, to be determined in advance by other calculations, model tests, etc., while η_n is to be selected so as to provide the correct moment. If the viscous moment on the tank is negligible, then $\eta_n = 0$.

FIGURE 1. HORIZONTAL BAFFLE ARRANGEMENT

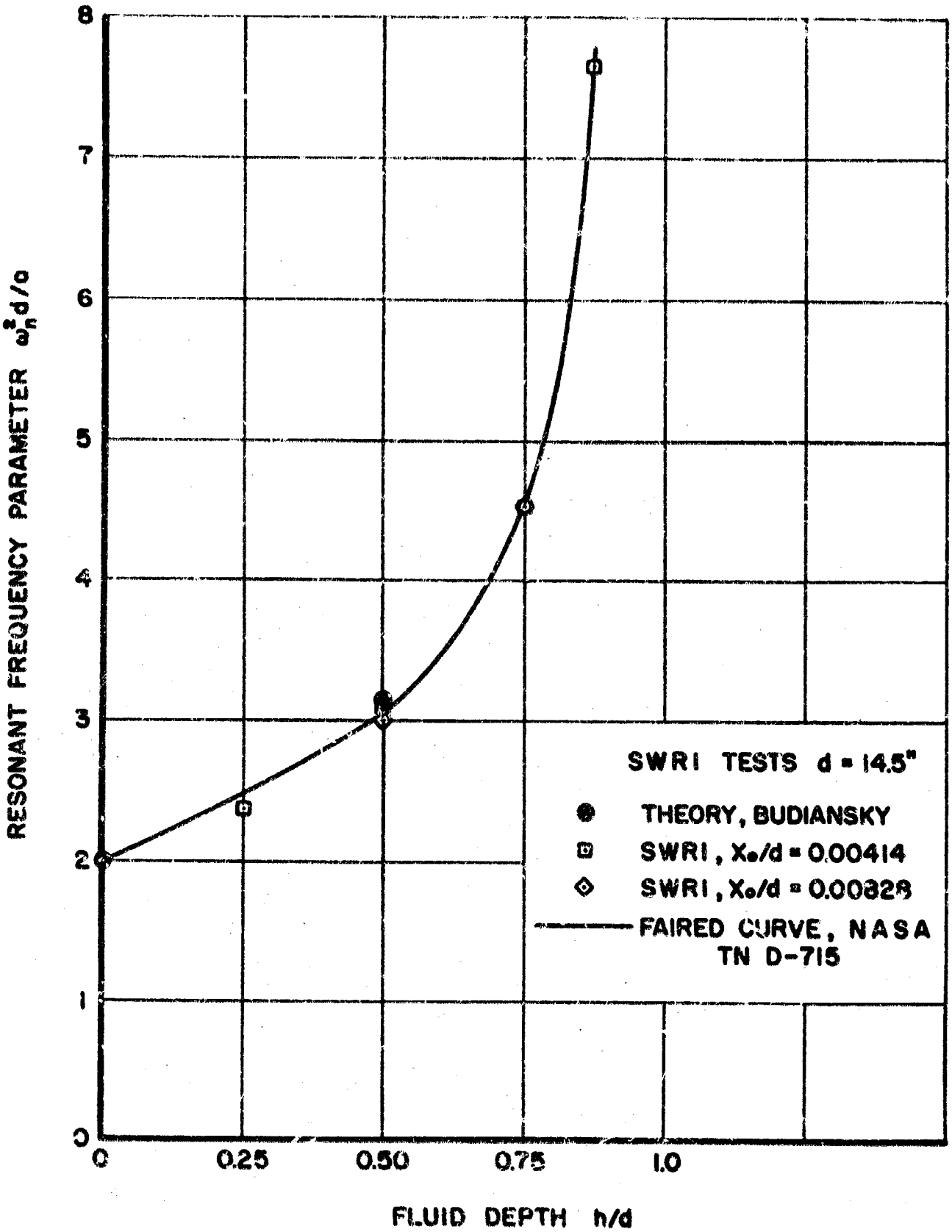

FIGURE 2 LIQUID FUNDAMENTAL RESONANT FREQUENCY VARIATION WITH DEPTH

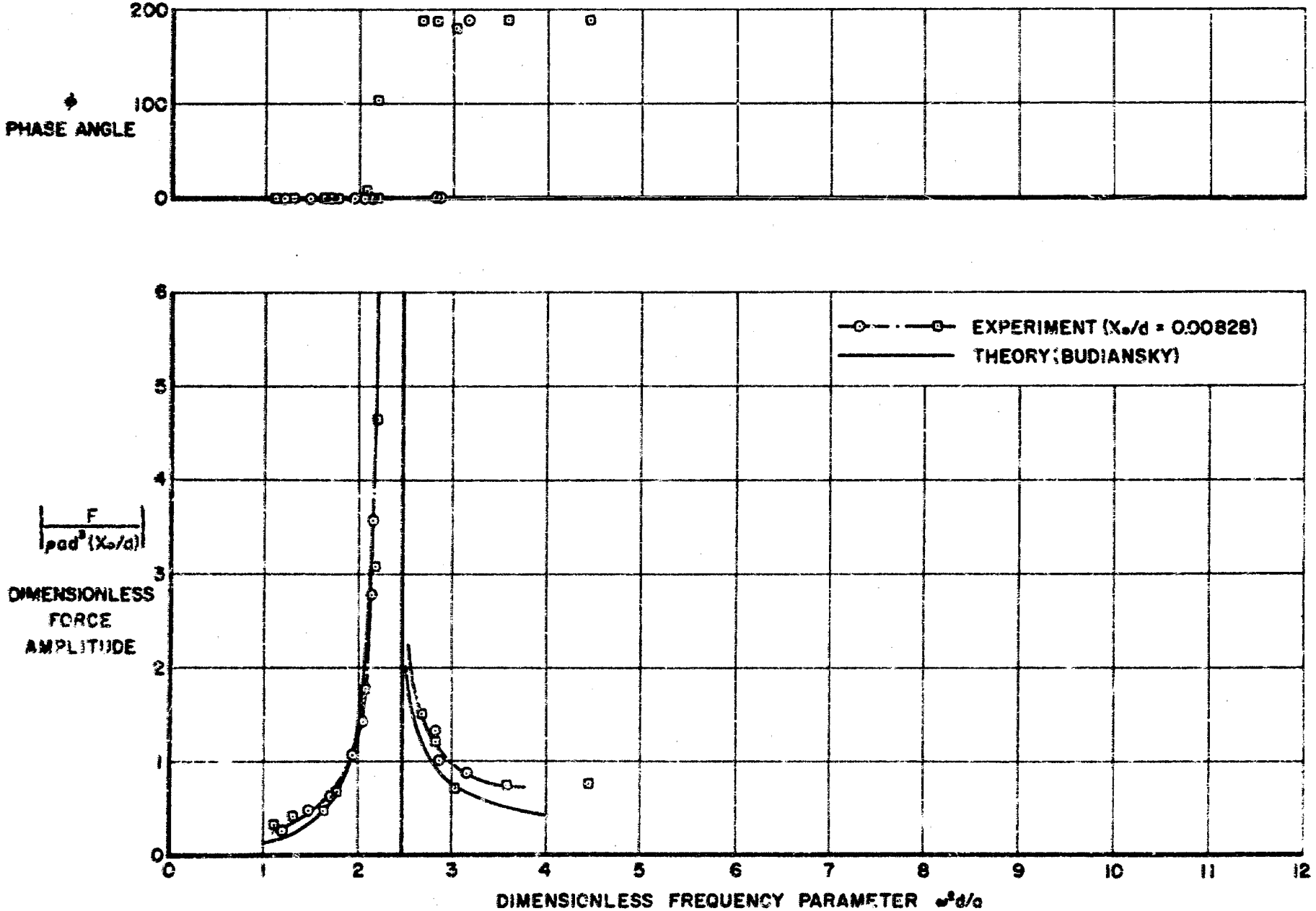

FIGURE 3 LIQUID TOTAL FORCE RESPONSE, UNBAFFLED TANK (h/d = 0.250)

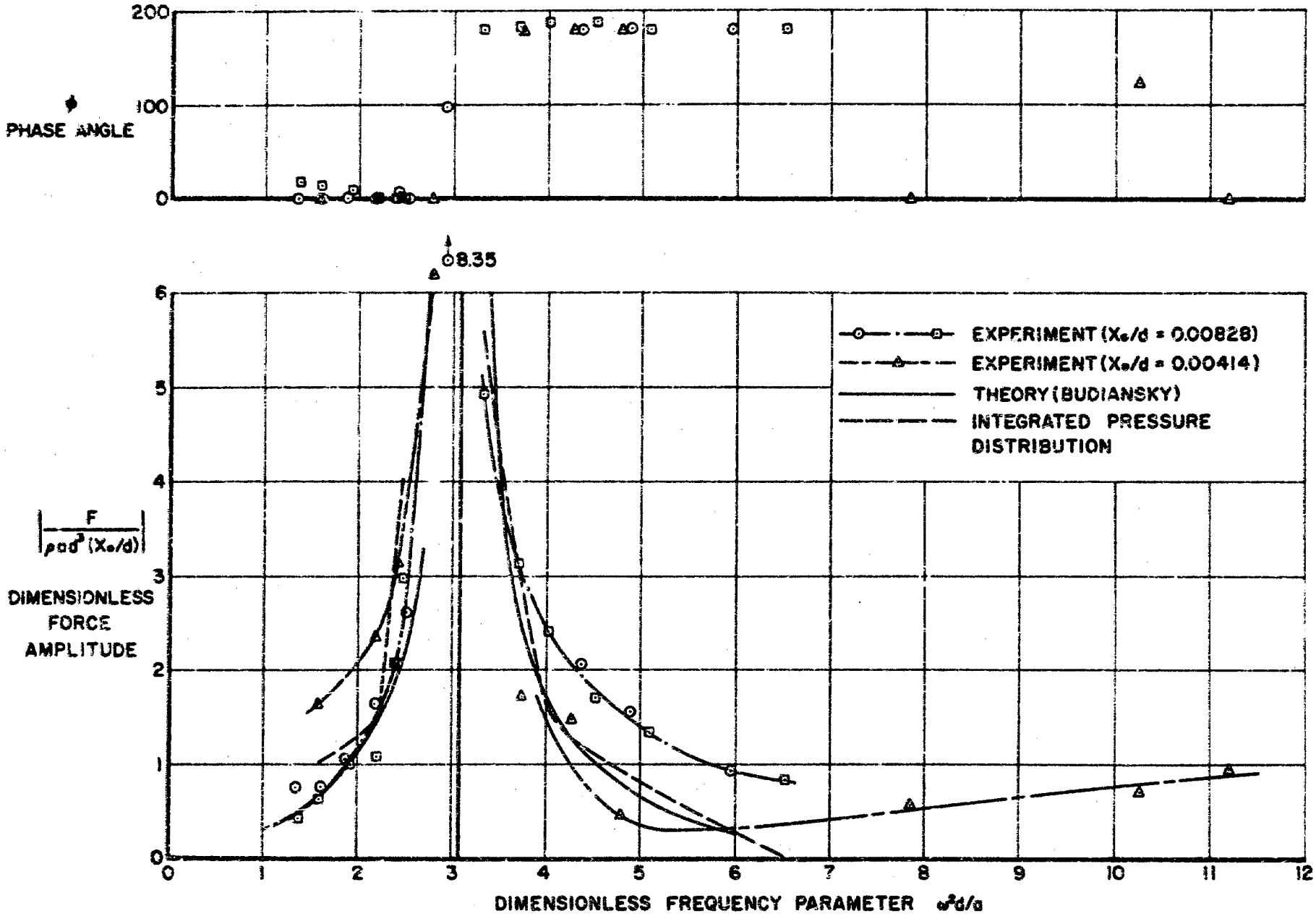

FIGURE 4 LIQUID TOTAL FORCE RESPONSE, UNBAFFLED TANK (h/d = 0.500)

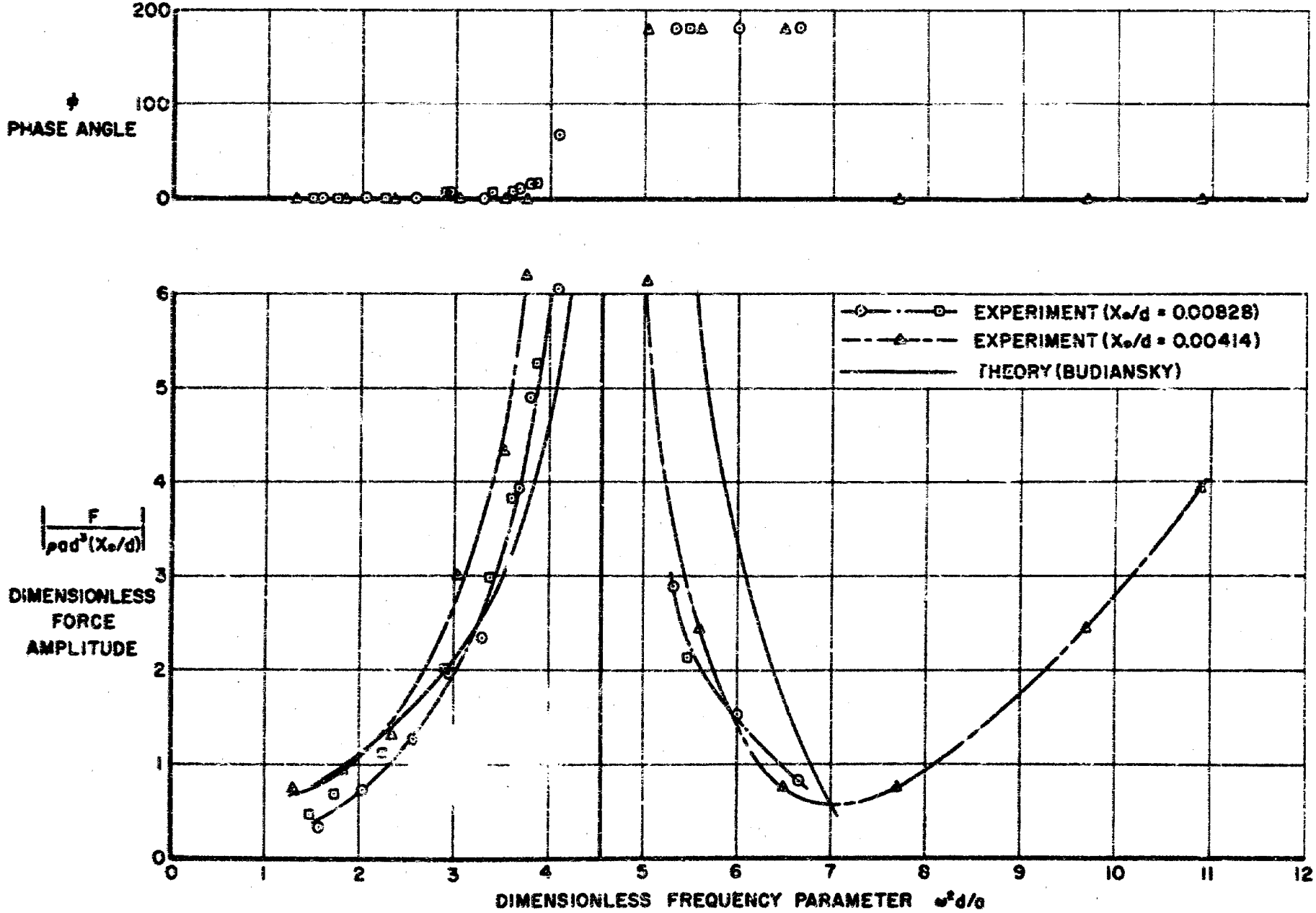

FIGURE 5 LIQUID TOTAL FORCE RESPONSE, UNBAFFLED TANK (h/d = 0.750)

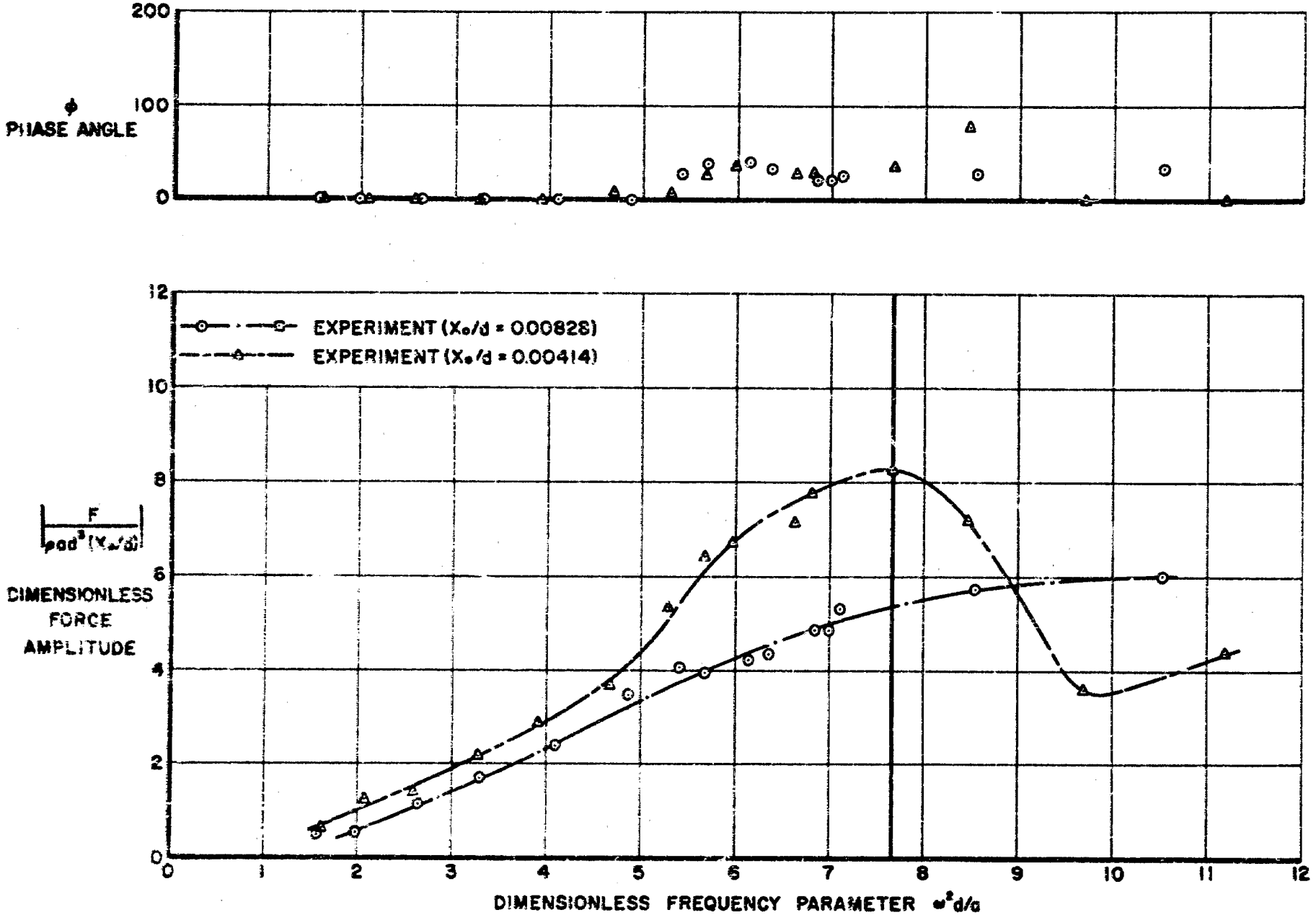

FIGURE 6 LIQUID TOTAL FORCE RESPONSE, UNBAFFLED TANK (h/d = 0.875)

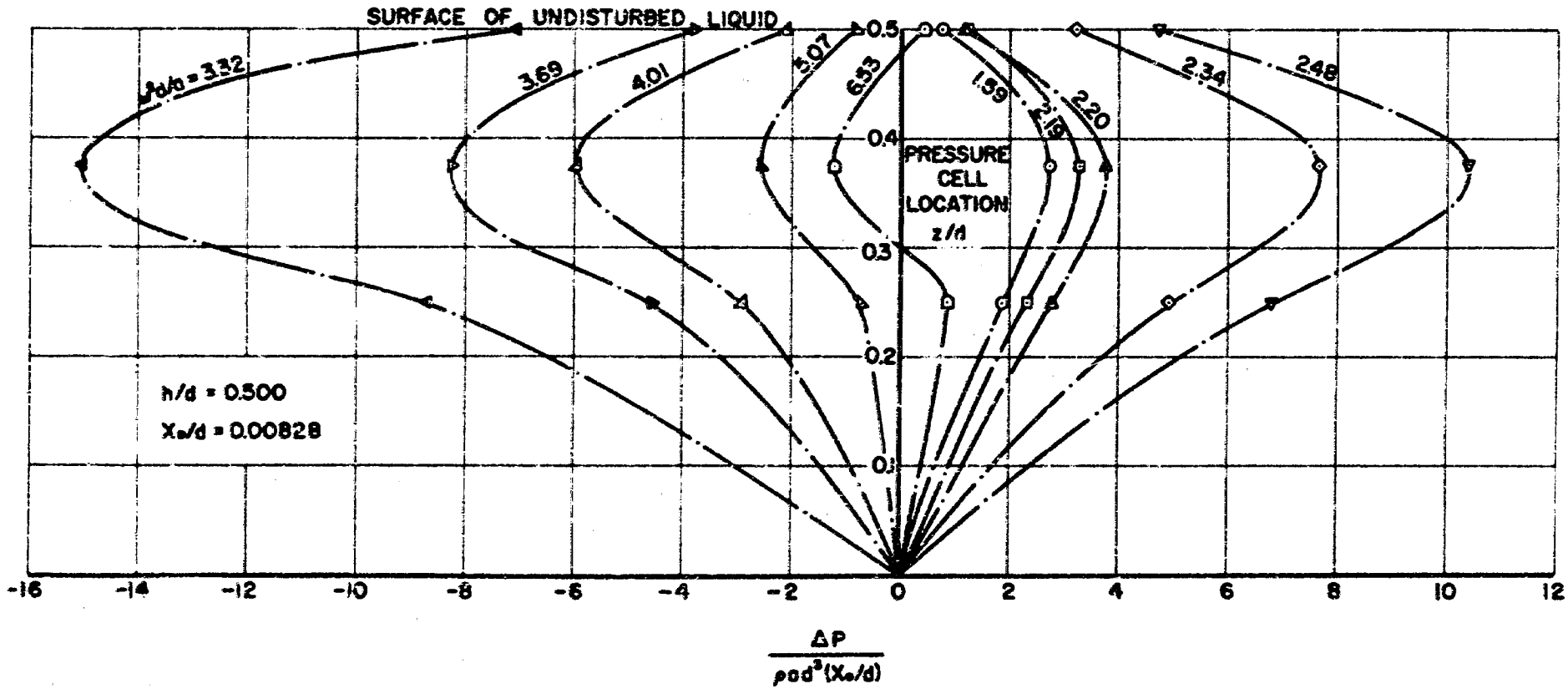

FIGURE 7 LIQUID WALL PRESSURE DISTRIBUTION, UNBAFFLED TANK

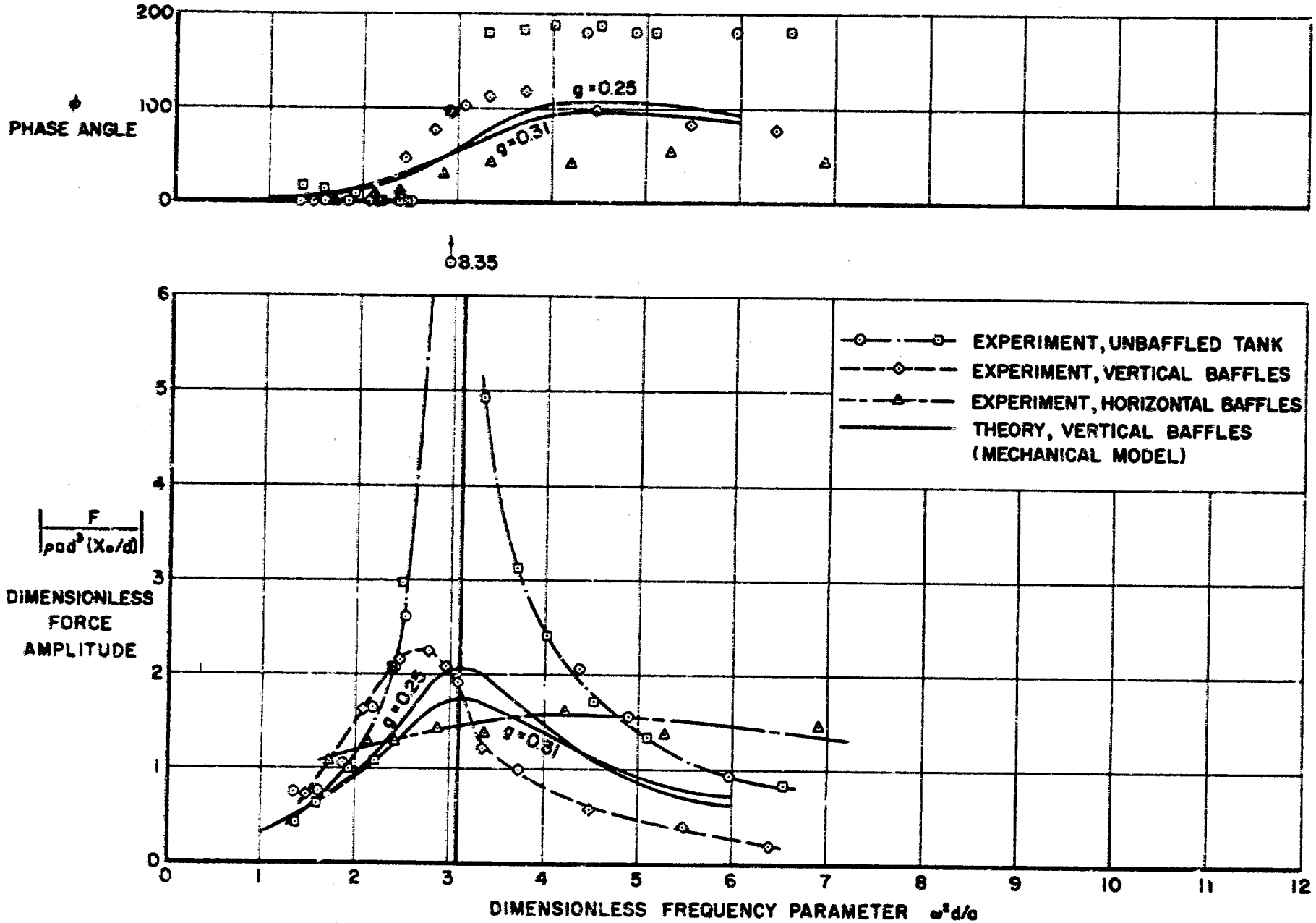

FIGURE 8 LIQUID TOTAL FORCE RESPONSE, BAFFLED TANK ($h/d = 0.500$, $X_o/d = 0.00828$)

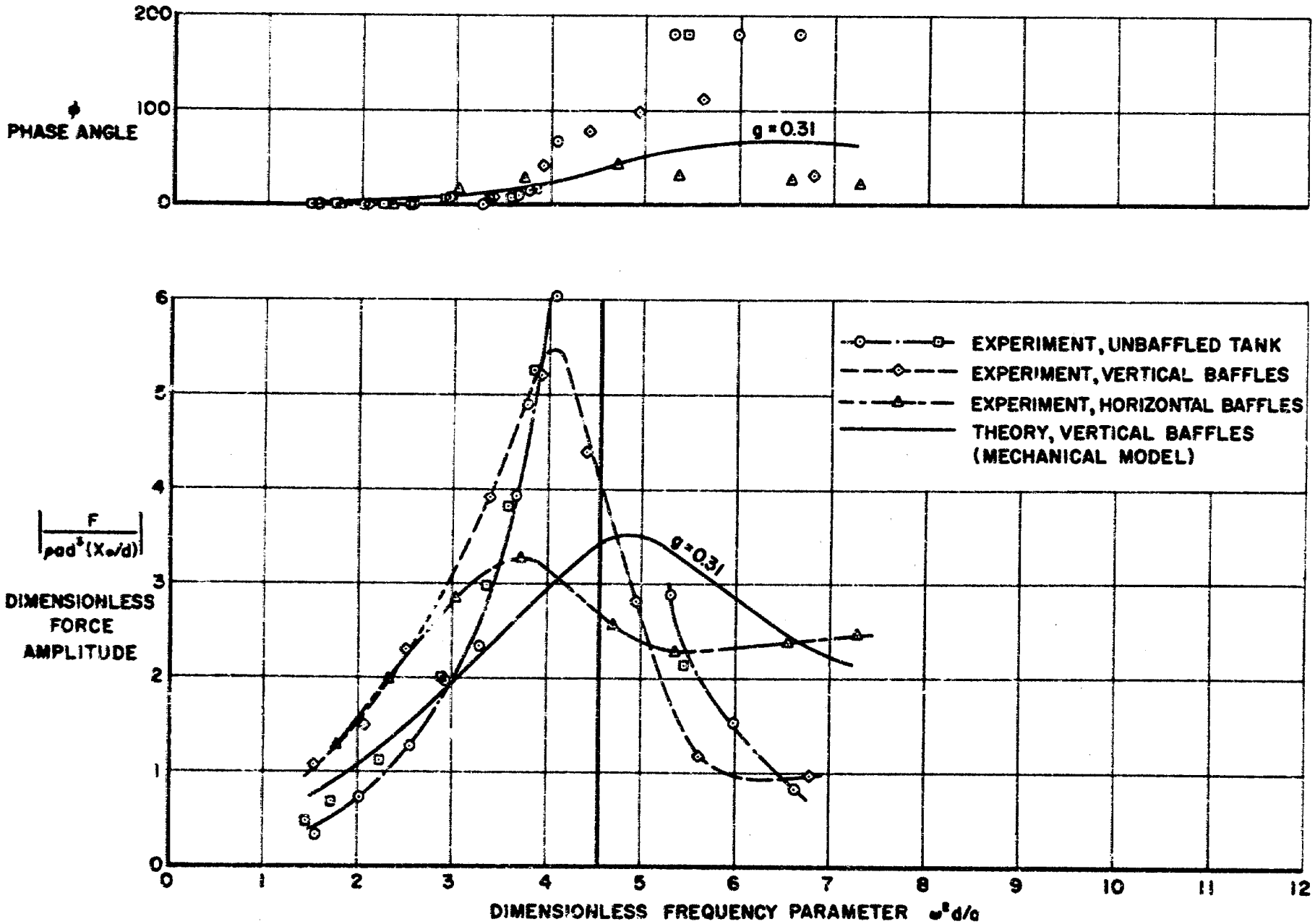

FIGURE 9 LIQUID TOTAL FORCE RESPONSE, BAFFLED TANK (h/d = 0.750, X_0/d = 0.00828)

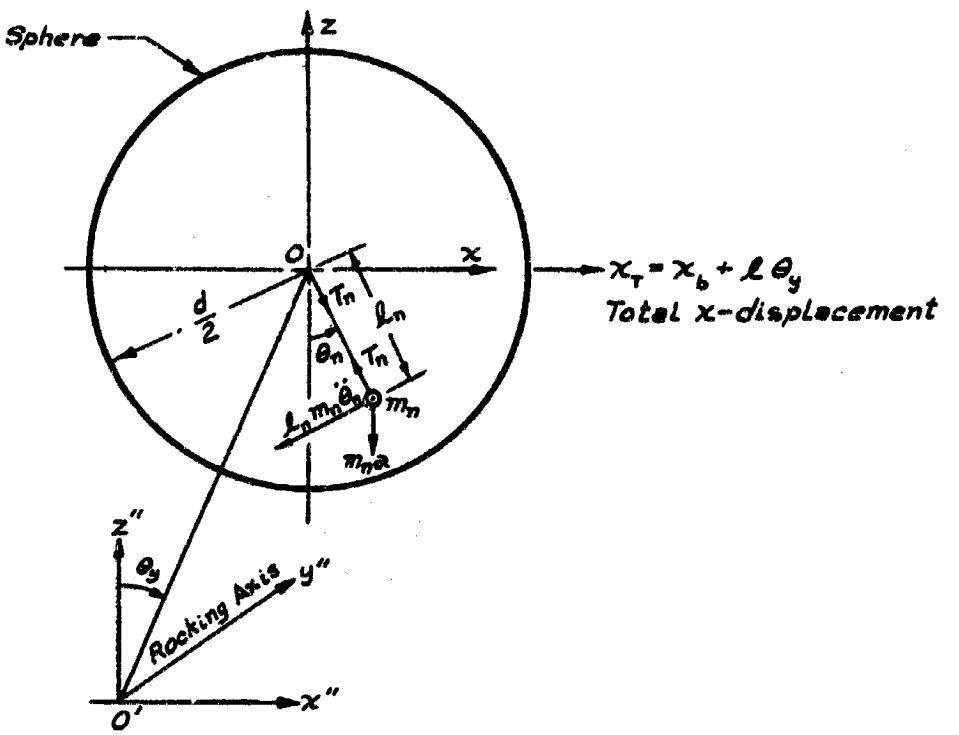

FIGURE A-1 ANALYSIS OF A SUSPENDED PENDULUM

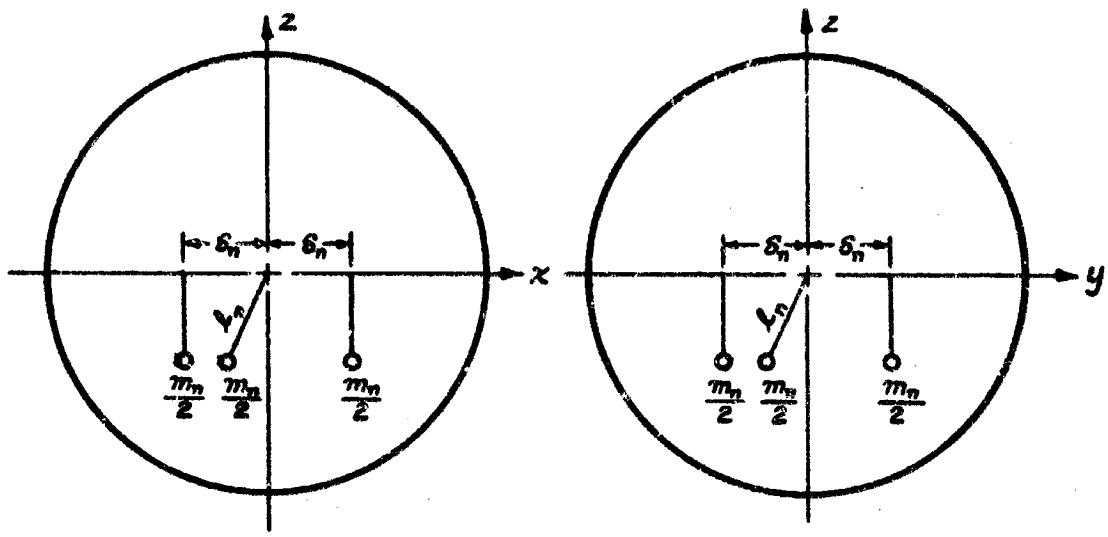

FIGURE A-2 EQUIVALENT MECHANICAL SYSTEM